DEUTSCHES ELEKTRONEN-SYNCHROTRON DESY

DESY 82-051
August 1982

ELECTROWEAK EFFECTS IN e^+e^- ANNIHILATIONS

by

B. Naroska

NOTKESTRASSE 85 · 2 HAMBURG 52

To be sure that your preprints are promptly included in the
HIGH ENERGY PHYSICS INDEX ,
send them to the following address (if possible by air mail) :

DESY
Bibliothek
Notkestrasse 85
2 Hamburg 52
Germany

DESY 82-051
August 1982

Electroweak Effects in e^+e^- Annihilations

B. Naroska
Deutsches Elektronen-Synchrotron DESY, Hamburg

Invited talk given at the 2nd International Conference on Physics in Collisions, Stockholm, June 1982

1. Introduction

After the discovery of weak neutral currents in neutrino scattering in 1973 (1) the study of the weak neutral current progressed rapidly. Data on neutrino scattering off electrons and nuclei all confirmed the so-called "Standard Model" of the unification of electromagnetic and weak forces by Glashow, Salam, and Weinberg (2). The famous electron-deuterium scattering experiment at SLAC (3) further confirmed these ideas by detecting the presence of a small parity violating amplitude. The neutrino experiments and the SLAC ed experiment were characterized by relatively low spacelike momentum transfers squared of a few eV^2 to at most a few 100 GeV^2.

With the advent of the e^+e^--ring PETRA in 1979 another powerful tool was available to test ideas about electroweak interaction in a different kinematical regime; the values of momentum transfer squared at the PETRA and PEP rings are more than a thousand GeV^2 (timelike). Also here one has the opportunity to study the neutral weak current in purely leptonic reactions $e^+e^- \to \ell^+\ell^-$, where ℓ stands for a charged lepton, namely e, μ or τ. In these processes there are no complications of nuclear or hadronic effects and a clean comparison with the results of the other purely leptonic reaction, neutrino scattering on electrons, is possible.

I shall report on the evidence we have now (i.e. June 1982, nearly three years after PETRA came into operation, and after 1.5 years of PEP operation) on electroweak interference effects in e^+e^- interactions. Data come mainly from 4 experiments at PETRA, namely CELLO, JADE, MARK J, and TASSO. Each experiment has collected data corresponding to approximately 60 pb^{-1} (except CELLO which has not been in the beam all the time), although not all experiments have yet analysed their data completely. The data were mostly taken around a cms energy of 34 GeV. Running at this energy will continue until the end of summer 1982, so the final statistics for this round of experiments will only be available toward the end of 1982. Data from PEP come from 2 experiments, MAC and MARK II at cms energy of 29 GeV. MARK II has about 40 pb^{-1} on tape, half of which is analysed.
For descriptions of the detectors see references (4) and (5) and references therein.

2. The Total Cross Section for $e^+e^- \to \mu^+\mu^-$

In e^+e^- annihilation at present energies we can observe the interference term of the electromagnetic and the weak amplitudes (Fig. 1). As we (still) have unpolarized beams and do not measure the polarization of the final leptons, we observe the parity conserving part of the interference term rather than the parity violating part observed in ed scattering. The total cross section for $e^+e^- \to \mu^+\mu^-$ for the electromagnetic interaction alone is, to lowest order:

$$\sigma_{\mu\mu} = \sigma_{pt} = \frac{4\pi\alpha^2}{3s}, \qquad \alpha = \frac{e^2}{\hbar c} \tag{2.1}$$

Throughout this report we shall use the ratio R of the cross section, either measured or predicted, to the pointlike cross section σ_{pt} derived in QED.

Including weak interactions and assuming just γ-Z_o mixing and e μ universality we get the following ratio (6):

$$R_{\mu\mu} = \frac{\sigma_{\mu\mu}}{\sigma_{pt}} = 1 + 2h_{VV}\,\chi + (h_{VV} + h_{AA})^2\,\chi^2. \tag{2.2}$$

h_{VV} and h_{AA} denote the vector and axial-vector coupling constants of the Z_o. The expression

$$\chi = \frac{G_F \cdot M_Z^2}{8\sqrt{2}\,\pi\alpha} \cdot \frac{s}{s - M_Z^2} \tag{2.3}$$

consists of two factors, the first one is the ratio of weak to electromagnetic coupling constants, the second one the ratio of the respective propagators. G_F is the Fermi coupling constant, $G_F \approx 10^{-5}/m_p^2$ and M_Z is the mass of the Z_o. If $M_Z \approx 90$ GeV then the weak propagator cannot be neglected any more at PETRA energies of $s = 1170\ \mathrm{GeV}^2$, where $M_Z^2/(s-M_Z^2) = -1.17$. The value of χ is with these parameter values $\chi = -0.061$.

In order to obtain numerical predictions for the coupling constants and the Z_o mass, one has to work with a specific model. In the standard model there is only one Z_o and therefore one has factorization of the coupling constants. Using again eμ universality, one can write:

$$h_{VV} = v_e \cdot v_\mu = v^2 = (-1 + 4\sin^2\theta_w)^2$$
$$h_{AA} = a_e \cdot a_\mu = a^2 = (-1)^2 \tag{2.4}$$

The only parameter in this model is $\sin^2\theta_w$, the (γ, Z_o)-mixing parameter, which not only determines the value of h_{VV} but also of the mass of the Z_o. A value of $\sin^2\theta_w = 0.23$, which was determined at low Q^2 (7), gives $h_{VV} = 0.006$ and $M_Z = 88.6$ GeV. This very small vector coupling constant leads to practically unmeasurable effects in the total cross section. The second and third term in 2.2 are at $s = 1170\ \mathrm{GeV}^2$ $-7 \cdot 10^{-4}$ and $38 \cdot 10^{-4}$ respectively.

Given this small expected deviation of the total cross section from QED of less than 0.5%, and given the statistical and systematic errors of the experimental data, a test of QED also constitutes a test of the standard electroweak model. In Fig. 2 the total measured cross section divided by the QED cross section is given as a function of energy. The straight line at 1 represents the prediction of QED and to a very good approximation also of the standard model with $\sin^2\theta_W = 0.23$. The agreement of the data points from the PETRA experiments with this line is good within errors. The deviations of the measurements of the total cross section from QED are traditionally parametrized by cut off parameters Λ:

$$R_{\mu\mu} = 1 \pm \frac{2s}{\Lambda_\pm^2}$$

The experiments obtain lower limits for Λ around 150 GeV at the 95% confidence level. The lines corresponding to this value are given in Fig. 2. The pointlike nature of QED has therefore been verified to distances of about $1.3 \cdot 10^{-16}$ cm.

The fact that the weak amplitude with currently known parameters does not give a measurable effect in the total cross section does not mean that nothing can be said about it. If we assume the unification idea is correct, then limits on the coupling constants h_{VV} and h_{AA} can be derived. For these

the s-dependence is important as can be seen from the dash-dotted line in Fig.2. This line was obtained using the vector dominant solution for the weak couplings, namely $v^2 = 1$ and $a^2 = 0$, which was one possible solution after the νe experiments. The s-dependence of this solution is not favoured by the data. The determination of the coupling constants will be discussed in section 4.

3. The Angular Distribution of μ-Pairs

3.1 The Asymmetry

The differential cross section for $e^+e^- \to \mu^+\mu^-$ assuming $\gamma - Z_0$ mixing has the following form (notation as in section 2):

$$\frac{d\sigma}{d\Omega} = \frac{\alpha^2}{4s}\left(F_1\,(1 + \cos^2\theta) + F_2 \cos\theta\right)$$

$$F_1 = 1 + 2h_{VV}\chi + (h_{VV} + h_{AA})^2\,\chi^2 \qquad 3.1$$

$$F_2 = 4h_{AA}\chi + 8h_{VV}h_{AA}\,\chi^2$$

θ is the angle between the μ^+ and the positron beam direction. The cross section contains a term proportional to $\cos\theta$, which leads to a forward backward asymmetry A:

$$A = \frac{3}{8}\,\frac{F_2}{F_1} \approx \frac{3}{2}\,h_{AA}\,\chi \qquad 3.2$$

The magnitude of A is determined entirely by the axial coupling constant h_{AA} for a fixed Z_0 mass. For $s = 1170\ \text{GeV}^2$, $M_z = 90$ GeV and $h_{AA} = 1$ an asymmetry of $A = -9.2\%$ is predicted by the standard model. Before the experiments had enough data to fit the angular distributions it was customary to quote an asymmetry $A = \frac{N_F - N_B}{N_F + N_B}$, where N_F and N_B are the number of μ^+ emitted into

the forward and backward cone, respectively. This asymmetry depends on the acceptance of the individual experiment. Therefore they now prefer to fit the angular distribution and calculate it according to 3.2.

3.2. Event Selection

The event selection procedures of all groups (8,5) are designed to reduce the background in the μ pair sample to a negligible fraction, keeping a high efficiency. The details in the various experiments are different, so here we give just the general principles.

Pairs of tracks are selected which are collinear to within 10 - 20 degrees. The main background comes from Bhabha events, cosmic ray muons, the two photon process $e^+e^- \to ee\mu\mu$, and τ pairs. The non-muon background is eliminated using particle identification by muon filters and shower counters. Cosmic rays are recognized by their different time-of-flight. The two photon events are eliminated by demanding that both muons have high energy. τ pairs, where both taus decay into a muon lead to a background that cannot be eliminated, which, however, is small for the experimental cuts used, of the order of 1 - 2%. Furthermore the angular distribution of taus is expected to be modified by the weak current in the same way as that of μ pairs. In general one can say that background would either reduce or leave unaffected any existing asymmetry from electroweak interaction, but would not artificially induce one.

3.3. Radiative Corrections

Until now we have only considered the lowest order diagrams of Fig. 1. Higher order effects exist in principle for both interaction types, the electromagnetic and the weak.

The diagrams contributing up to order α^3 to the purely electromagnetic process (Fig. 3a) were calculated using the programs by Berends and Kleiss (9).

The magnitude of the correction depends on the cuts applied to the data; in Fig. 3b an example for a particular set of cuts is given as a function of cosθ. The correction definitely has an angular asymmetry. The data are corrected for this asymmetry, so that any remaining asymmetry is due to the electroweak effect. The correction applied to the data is given in column 5 of Table 1.
The acollinearity distribution of the final state particles is a check of radiative corrections. It has previously been examined for Bhabha scattering (10) and has now been obtained for final state muons by the MARK J and MARK II detectors. The MARK J distribution is shown in Fig. 4. The agreement of data points with calculations is good within errors.

In principal higher orders have to be taken into account also for the weak diagram. But the modification of the forward backward asymmetry is still expected to be small at present energies (11,12).
Up to now calculations only exist for a limited number of diagrams (11), which include hard photon emission in the initial state. This leads to a decrease of the expected asymmetry of -9.5% to -(8.7 ± 0.5)% for the MARK J experiment, mainly by decreasing the effective cms energy.
Calculations of the vacuum polarization of the Z_0 are still missing. They might counteract the decrease of the expected asymmetry by raising the weak amplitude (12).

3.4. Results

In Fig. 5a the angular distribution of the four PETRA experiments are displayed. The full lines show a fit allowing for an asymmetry, $F(\cos\theta) = N(1 + \cos^2\theta + q \cdot \cos\theta)$. The dotted line shows the symmetric prediction by QED, where only the normalization was fit.

In all distributions (except the CELLO one, which has considerably larger errors than the others) a clear preference for the non-symmetric form is observed. In Fig. 5b similar distributions from the two PEP experiments are shown.

Table 1 contains a summary of the results at high energy. The measured asymmetry was derived from the fit parameters q according to 3.2 and is therefore independent of the individual acceptances. The 3 PETRA experiments JADE, MARK J and TASSO all measure an asymmetry that is at least 4 standard deviations away from 0. The averaged PETRA value - which is of course only meaningful if the systematic errors of the individual experiments are small - is -(11.9 ± 1.5)%, 8 standard deviations from 0. This value has to be compared to an expected asymmetry in the standard model of roughly -9.3%, calculated without radiative corrections for the weak diagram.

The expected asymmetry for the PEP experiments is only -6.2% due to their lower cms energy. Because of their error bars they are still compatible with no asymmetry, though also with the standard model.

The PETRA experiments also took data at lower energies. The energy dependence of the integrated forward backward asymmetry is displayed in Fig. 6. It agrees, within errors, with the energy dependence predicted by the standard model.

4. Determination of the Weak Coupling Constants and Mass of the Z_0

The non-zero asymmetry clearly demonstrates the presence of a weak neutral current, so it is meaningful to determine its couplings to the electron and muon.

The vector coupling constant is mainly determined by the total cross section (equation 2.2). The axial-vector coupling constant is determined by the asymmetry of the angular distribution (equation 3.2), but enters also in the total cross section. Because of this weak correlation the experiments usually perform combined fits to determine both coupling constants simultaneously. If the cross sections from Bhabha scattering are also used, more accuracy, mainly for the vector coupling constant, is obtained.

The numerical results of the various experiments are displayed in Table 2. They have already been divided by 4 to facilitate the comparison to

νe scattering. When several values appear for one experiment, they have been obtained with different input data, indicated in the third column. These results can be compared directly to the results of the νe experiments, if we assume that the coupling of the neutrino to the Z_o is unity (13). This is experimentally confirmed to ~20% from νe and ed scattering, and with much higher accuracy by comparing neutral and charged currents in deep inelastic scattering off nuclei. We assume that the following relations hold:

$$h_{VV} = 4g_V^2$$

$$h_{AA} = 4g_A^2$$

where g_V and g_A are the couplings measured in νe scattering. (The factor 4 comes in because of the way we defined our expression χ).
In Fig. 7 the results of the e^+e^- experiments (the best value of each group) are plotted in a g_V^2, g_A^2 plane. One sees that, although the error bars are large, the measurements do cluster around g_V^2 close to 0 and g_A^2 close to 1/4.

In νe scattering two possible solutions are obtained and are indicated in Fig. 7 by the shaded areas. The e^+e^- measurement uniquely identifies the axial dominant solution as the correct one, a result which previously had been obtained by information from the ed scattering experiment. The numerical values of this solution are also given together with the predictions of the standard model in the last two rows of table 2.

A limit on the mass of the neutral vector boson Z_o can be derived using the measured asymmetry and assuming that $h_{AA} = 1$ as in the standard model. The averaged PETRA asymmetry then leads to $M_Z = 60^{+11}_{-6}$ or, at the 95% confidence level to $50 < M_Z < 106$ GeV. The evidence for a finite Z mass is not very strong yet, because the measured asymmetry is only 2.6 standard deviations from the predicted value $A = -0.079$ for $M_Z = \infty$.

5. Production of τ Pairs

If generation universality holds the same effects that have been observed in μ pair production would be exptected in τ pair production. There are models, however, based on a composite quark and lepton picture, that predict

a different behaviour of taus from muons (14).

The analysis of τ pairs has not yet reached the same level of accuracy as that of μ pairs. This is due to the fact that taus decay before they enter the detector and the neutrinos leave the detector unobserved, which makes the event recognition and background rejection more difficult. Some groups have restricted their analysis to special decay channels, which reduces statistics. The amount of data available for the various groups is given in Table 3 (15).

In Fig. 8 the total cross section ratio for τ pairs is plotted as a function of energy (note the different scale from Fig. 2!). The errors contain statistical as well as systematic errors. For the TASSO data the error of 16% for the branching fraction of their analysed channel is included as well.

As for the muon data the τ total cross section agrees with the QED prediction, which also means agreement with the standard model as explained in chapter 2. The angular distributions of all 4 PETRA and 2 PEP experiments are displayed in Figs. 9a and b. Again asymmetric and symmetric fits to the data are shown (full and dotted curves respectively). The data do not unambiguously show a preference for a negative asymmetry like the muon data. The JADE and TASSO data look quite symmetric, and MAC even gets a positive asymmetry. Numerical results are summarized in Table 3. More data and complete analysis of existing data will hopefully clarify the situation in the near future.

6. $e^+e^- \to$ Hadrons

In the quark parton model hadron production proceeds via a quark antiquark pair, $q_f\bar{q}_f$. At present cms energies 5 different quark flavours contribute: u, d, s, c, and b. Studying the electroweak interactions in e^+e^- annihilation offers the unique possibility of testing the couplings of the Z_o to the heavy quarks, which cannot easily be done in fixed target experiments.

It has not yet been possible to determine the forward backward asymmetry of quarks. Instead the determination of the weak coupling constants is

restricted to analysing the total cross section ratio:

$$R = \sigma_T/\sigma_{pt} = 3\sum_f R_{ff} = 3\Sigma_f[Q_f^2 + 2Q_f v_e v_f \chi + (v_e^2 + a_e^2)(v_f^2 + a_e^2)\chi^2] \qquad 6.1$$

where v_e, v_f, a_e, and a_f denote the vector and axial vector coupling constants to the electron and q_f respectively. The expected change in the total cross section due to the neutral weak current is larger than for lepton pairs due to the larger vector coupling constants (Table 4). The comparison of 6.1 to the data is more complicated, though, because the electroweak interference is not the only modification of the simple quark parton model; substantial effects are expected by first and second order QCD.

In ref.16, R was calculated including QCD corrections and the electroweak contributions. The QCD coupling constant is $\alpha_s = 12\pi/(33-2N_f)/\ln(s/\Lambda^2)$ with $N_f = 5$ and $\Lambda = 0.3$ GeV, which gives $\alpha_s = 0.17$ at the highest PETRA energy. Non-zero quark masses were also taken into account, which gives a modification at the threshold mainly.

The predictions of the naive quark parton model (lower dashed line), QCD (upper dashed line), and QCD including weak contributions (full lines for 3 values of $\sin^2\theta_w$) are displayed in Fig. 10.

The experimental data from JADE, MARK J, and TASSO (17) are shown in Figs. 10a, b and c. Their results for $\sin^2\theta_w$ - fixing Λ to 0.3 - are 0.24 ± 0.05, $0.48^{+0.09}_{-0.25}$, and $0.40 \pm 0.15 \pm 0.08$, respectively. In these results the overall normalisation error of roughly 5% was taken into account and, for MARK J and TASSO, also a point-to-point normalisation error.The wide range of results reflects the low sensitivity of the total cross section to small changes in $\sin^2\theta_w$. On the other hand the data exclude values below about 0.15 and above about 0.60 and therefore agree with the values obtained in low energy neutrino scattering on light quarks (7).

7) Summary

Data on e^+e^- annihilation into $\mu^+\mu^-$, $\tau^+\tau^-$, and $q\bar{q}$ were used to test electroweak theories up to an $s \sim 1200$ GeV^2. The following results were obtained:

1) The PETRA experiments clearly demonstrated a forward backward asymmetry in the angular distribution of μ pairs. The combined value is $A = -(11.9 \pm 1.5)\%$ to be compared to -9.3% predicted by the standard model using $\sin^2\theta_w = 0.23$.
   The PEP experiments agree with this result, although they are also compatible with pure QED due to their lower cms energy and larger errors.
2) The angular distributions of τ pairs are compatible with the standard model but also with pure QED due to larger errors.
3) The total cross sections, both for μ and τ pairs, agree with QED and the standard model, which for $\sin^2\theta_w = 0.23$, still coincides with QED at present energy.
4) The weak coupling constants were determined, the average PETRA values are $h_{VV}/4 = -0.01 \pm 0.03$ and $h_{AA}/4 = 0.33 \pm 0.04$. This result picks out one of the two solutions obtained in νe scattering and ed scattering results.
5) The total cross section for the production of hadrons was analysed in the framework of the quark parton model, taking into account QCD corrections and weak contributions using the standard model. The data agree with the predictions using $\Lambda_{QCD} = 0.3$ (which corresponds to $\alpha_s = 0.17$ at cms energy of 34 GeV) and $\sin^2\theta_w = 0.23$.

Acknowledgement

I am grateful to the organisers of the conference, especially P. Carlson, for inviting me and for their warm hospitality and friendly help.
I wish to thank the members of the CELLO, MARK J, TASSO, MAC, and MARK II collaborations for providing me with their partly still unpublished data.
Special thanks to A. Böhm, J. Dorfan, P. Grosse-Wiesman, and U. Martyn for discussing the details of the data.
I thank my JADE colleagues P. Dittmann, R. Marshall, and P. Steffen for help during the preparation of the talk and the manuscript.

References

1) F. Hasert et al., Phys. Lett. 46B (1973) 121 and 138

2) S.L. Glashow, NP 22 (1971; Rev. Mod. Phys. 52 (1980) 539
A. Salam, PR 127 (1962) 331; Rev. Mod. Phys. 52 (1980) 525
S. Weinberg, PRL 19 (1967) 1264; Rev. Mod. Phys. 52 (1980) 515

3) C.Y. Prescott et al., Phys. Lett. 77B (1978) 347; 84B (1979) 524

4) H.J. Behrend et al., Phys. Scripta 23 (1981) 610
W. Bartel et al., Phys. Lett. 88B (1979) 171
MARK J Coll., Phys. Reports 63 (1980) 339
R. Brandelik et al., Phys. Lett. 83B (1979) 261; 92B (1980) 199

5) J.G. Smith, SLAC-PUB-2921 and Proc. of XVII Rencontre de Moriond, Les Arcs, 1982 to be published
J. Dorfan, SLAC-PUB-2813 (1981), SLAC Summer Inst.

6) R. Budny, Phys. Lett. 55B (1975) 227

7) J.E. Kim et al., Rev. of Mod. Phys. 53 (1981) 211

8) W. Bartel et al., Phys. Lett. 108B (1982) 140
H.J. Behrend et al., DESY 82-019 (1982)
R. Brandelik et al., Phys. Lett. 110B (1982) 173
B. Adeva et al., Phys. Rev. Lett. 48 (1982) 1701

9) F.A. Behrends, F.K.J. Gaemers and R. Gastman, Nucl. Phys. B63 (1973 381
F.A. Behrends, K.F.J. Gaemers and R. Gastman, Nucl. Phys. B68 (1974) 541
F.A. Behrends, and R. Kleiss, Nucl. Phys. B178 (1981) 141

10) W. Bartel et al., Phys. Lett. 92B (1980) 206
R. Brandelik et al., DESY 82-032, to be published ; Phys. Lett. 94B (1980) 259
B. Adeva et al., Phys. Rev. Lett. 48 (1982) 721

11) F.A. Behrends, R. Kleiss, and S. Jadach: Radiative Corrections to Muon Pair and Quark Pair Production in Electron-Positron Collisions in the Z_o Region, Preprint Instituut Lorentz, Leiden, and references therein

12) E.A. Paschos, private communication

13) J.J. Sakurai, in Proc. of XVII Rencontre de Moriond (to be published), and MPI-PAE/Pth 24/82
P.Q. Hung and J.J. Sakurai, Ann. Rev. Nvc. Sci, 31 (1981) 375

14) C.H. Albright et al., Phys. Lett. 113B (1982) 225

15) M. Nozaki, UT LICEPP 82-02
H.J. Behrend et al., DESY 82-020, 1982, to be published
MARK J, private communication
R. Brandelik et al., Phys. Lett. 110B (1982) 173

16) J. Jersak et al., Phys. Lett. 98B (1981) 363

17) W. Bartel et al., Phys. Lett. 101B (1981) 361 and private communication
R. Brandelik et al., DESY 82-010, to be published in Phys. Lett.
MARK J, private communication

Table 1: $e^+e^- \to \mu^+\mu^-$

Asymmetry for $e^+e^- \to \mu^+\mu^-$ at high energy for PETRA and PEP experiments. A_{QED} is the correction due to higher order diagrams (chapter 3.3), A is the measured asymmetry derived according to equation 3.2, corrected for A_{QED}. A_{GWS} is the expectation in the standard model using $\sin^2\theta_w = 0.23$.

EXP	$\int Ldt$ [pb^{-1}]	$\langle\sqrt{s}\rangle$ [GeV]	$N_{\mu\mu}$	A(%) QED	A(%) measured	A(%) GWS
CELLO	11.2	34.2	387	1.6 ± 0.5	-6.4 ± 6.4	-9.2
JADE	34.9	34.2	1590	1.3	-12.7 ± 2.7	-9.2
MARK J	48.3	34.6	2435	1.4 ± 0.5	-9.8 ± 2.3	-8.7 ± 0.6*
TASSO	35.4	34.2	1155	1.6 ± 0.5	-16.1 ± 3.2	-9.2
PETRA	130	34.4	5567		-11.9 ± 1.5	~ -9.3
MAC	20	29	1515	2.6	-3.2 ± 2.8	-6.3
MARK II	15.4	29	652		-9.6 ± 4.5	-6.3

Table 2: Weak Coupling Constants

The weak coupling constants obtained by PETRA and PEP experiments using leptonic data as input (column 2). M_Z = 90 GeV was assumed for the determination of h_{VV} and h_{AA}. The row marked Kim et al. gives a fit to the νe and ed data (7). In the last row the standard model prediction with $\sin^2\theta_w = 0.23$ is given.

EXP	DATA	$h_{VV}/4$	$h_{AA}/4$	$\sin^2\theta_w$
CELLO	μμ		0.17 ± 0.17	
CELLO	μμ,ττ,ee	-0.03 ± .11	0.31 ± 0.12	$0.21^{+0.14}_{-0.09}$
JADE	μμ	0.05 ± .05	0.37 ± 0.07	
MARK J	μμ	0.01 ± .08	0.28 ± 0.07	0.24 ± 0.11
TASSO	μμ	-.09 ± .11	0.45 ± 0.09	
TASSO	μμ,ee	-.04 ± .06	0.35 ± 0.09	$0.27^{+0.06}_{-0.07}$
PETRA (Average)		-.01 ± .03	0.31 ± 0.04	
MAC	μμ		0.13 ± 0.11	
MARK II	μμ		0.38 ± 0.18	
MARK II	μμ,ee	0.05 ± 0.10	0.24 ± 0.16	
Kim et al.	νe,ed	0.002 ± .005	0.29 ± .06	0.23 ± 0.01
GSW with $\sin^2\theta_w$=0.23		0.0016	0.25	

Table 3: High Energy Data on Tau Pair Production

Asymmetry for $e^+e^- \to \tau^+\tau^-$ at high energy for PETRA and PEP experiments. In column 5 the fraction of decays analysed are given. A is the measured asymmetry derived according to equation 3.2, corrected for A_{QED}. A_{GWS} is the expectation in the standard model using $\sin^2\theta_w = 0.23$.

Experiment	$\int Ldt$ (pb^{-1})	$\sqrt{s}$	$N_{\tau\tau}$	Fraction analysed (%)	Back-ground (%)	A(%) measured	A(%) GWS
CELLO	11.3	34.2	434	94	4	-10.3 ± 5.2	-9.2
JADE	17.4	34.4	569	70	4.5	-3.2 ± 5	-9.3
MARK J	50.2	34.6	550	30	5	-9 ± 6	-9.5
TASSO	35.8	34.3	262	38	2.7	-0.4 ± 6.6	-9.1
PETRA Average	114.7	34.4	1815			-6 ± 3	-9.3
MAC	7.0	29	242			4 ± 6	-6.3
MARK II	15.4	29	454			-3.9 ± 6	-6.3

Table 4: Weak Coupling Constants in the Standard Model

f	v_f	a_f	v_f^2 ($\sin^2\theta_w = 0.23$)
u,c	$1 - \frac{8}{3}\sin^2\theta_w$	1	0.15
d,s,b	$-1 + \frac{4}{3}\sin^2\theta_w$	-1	0.48
e,μ	$-1 + 4\sin^2\theta_w$	-1	0.006

Figure Captions

1) First order electromagnetic and weak processes contributing to $e^+e^- \to \mu^+\mu^-$.

2) Total cross section ratio for ee → μμ to the QED cross section as a function of s. The full line at $R_{\mu\mu} = 1$ gives the QED prediction and also the prediction of the standard model. The other curves are explained in the text.

3) a) Higher order diagrams taken into account for radiative corrections,
b) magnitude of radiative corrections for one particular set of cuts as a function of cosθ, displaying an angular asymmetry.

4) Acollinearity distribution for final state μ pairs obtained in the MARK J detector.

5) $s \cdot \frac{d\sigma}{d\Omega}$ for $e^+e^- \to \mu^+\mu^-$ for

a) PETRA experiments
b) PEP experiments

The curves are fits to the data:
—— $N(1 + \cos^2\theta + q \cdot \cos\theta)$ allowing for an asymmetry
---- $N'(1 + \cos^2\theta)$ symmetric

6) Integrated forward-backward asymmetry A as a function of s.

7) Weak coupling constants g_V^2 versus g_A^2. The shaded areas represent the one and two sigma overlap regions determined in the νe scattering experiments.

8) Total cross section ratio for τ pair production to the QED cross section.

9) Angular distributions of τ pairs for
a) PETRA experiments
b) PEP experiments
The curves are explained in Fig. 5.

10) Total cross section ratio for hadron production to the pointlike QED cross section from a) JADE, b) MARK J, and c) TASSO. The curves are explained in the text.

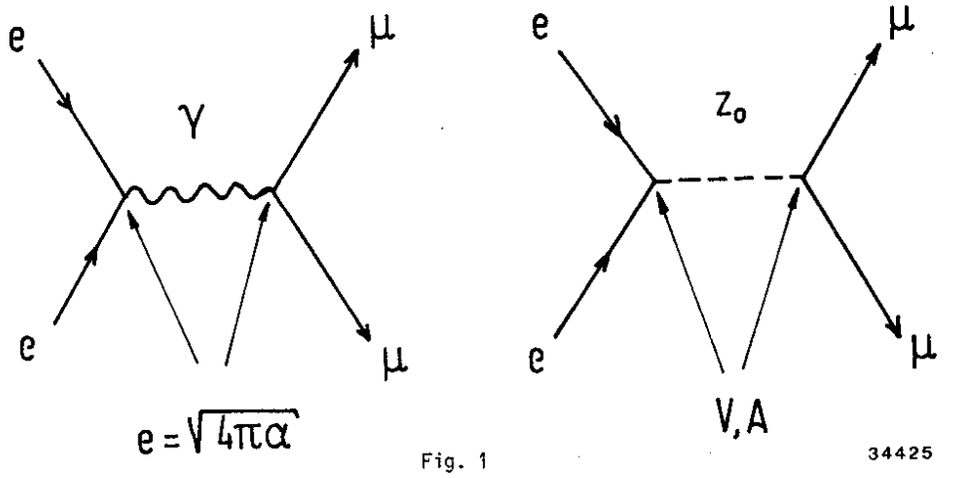
e
μ
γ
e
μ
e = √4πα
e
μ
Z₀
e
μ
V,A
34425

Fig. 1

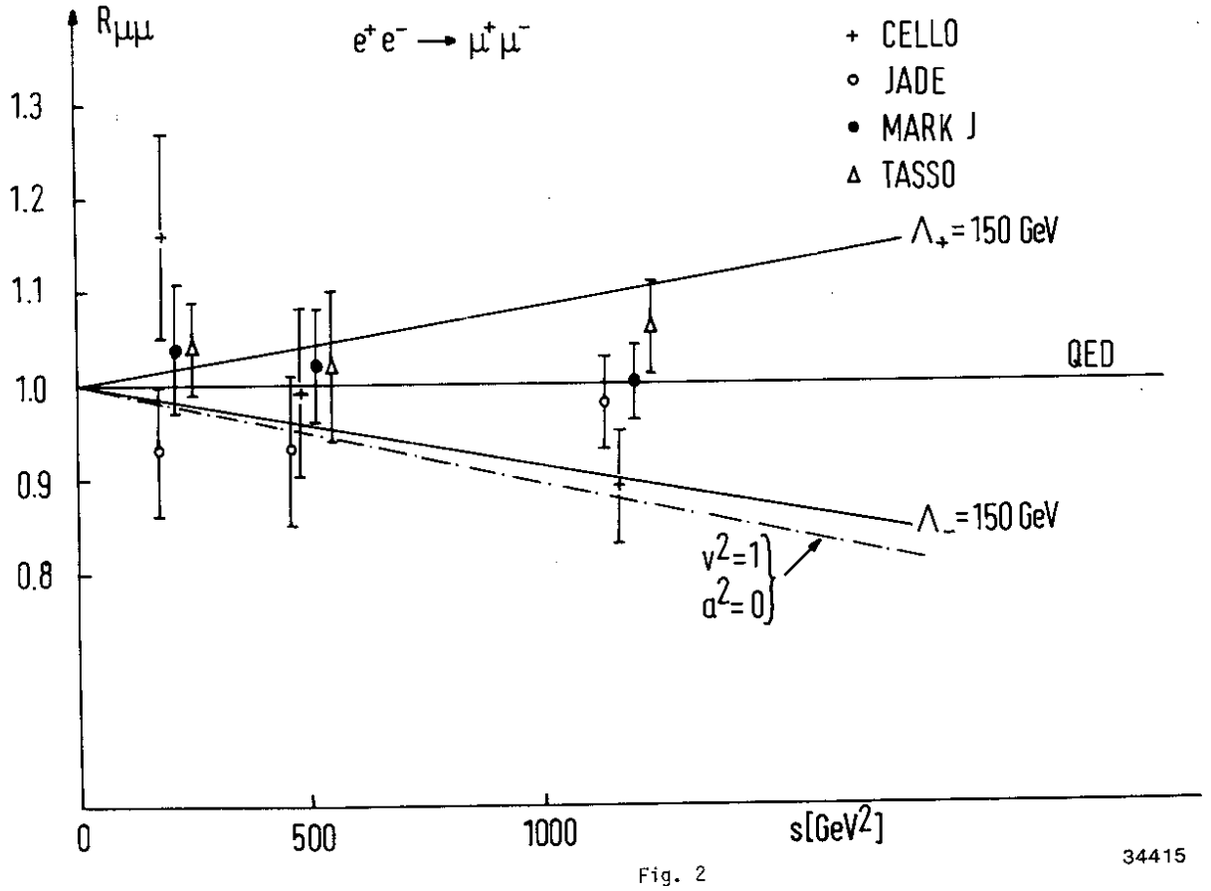
Rμμ
e⁺e⁻ → μ⁺μ⁻
+ CELLO
○ JADE
● MARK J
△ TASSO
1.3
1.2
1.1
1.0
0.9
0.8
Λ₊ = 150 GeV
QED
Λ₋ = 150 GeV
v² = 1
a² = 0
0
500
1000
s[GeV²]
34415

Fig. 2

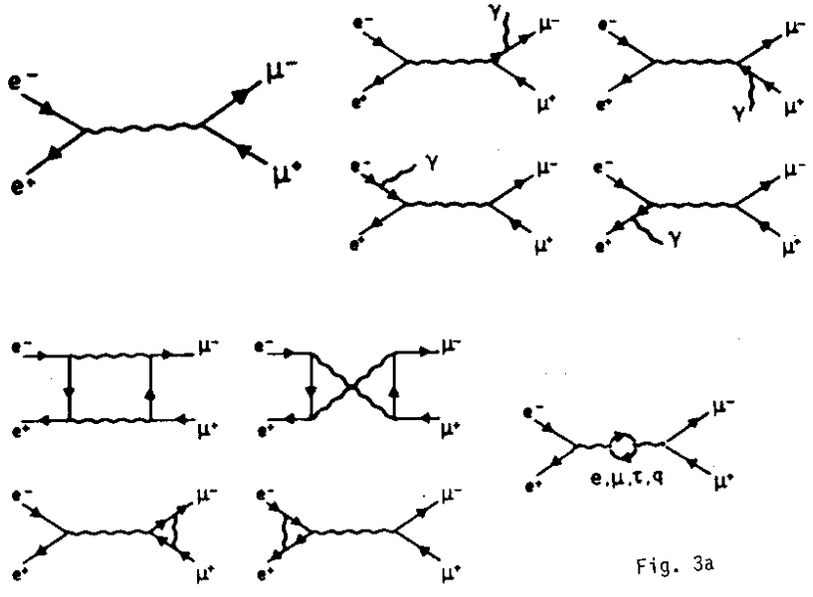

Fig. 3a

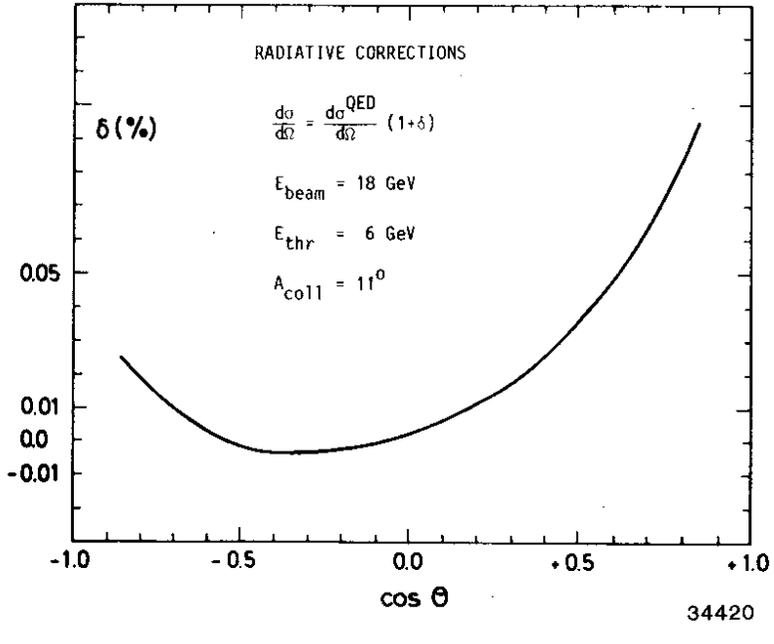

Fig. 3b

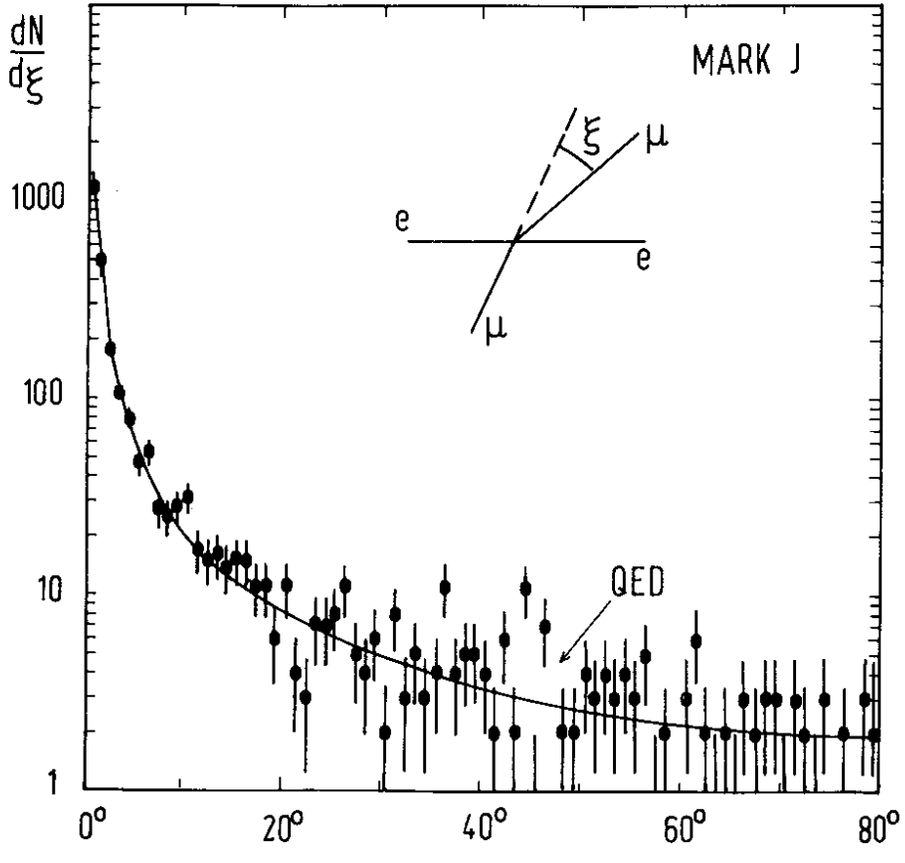

Fig. 4 acollinearity angle ξ

34418

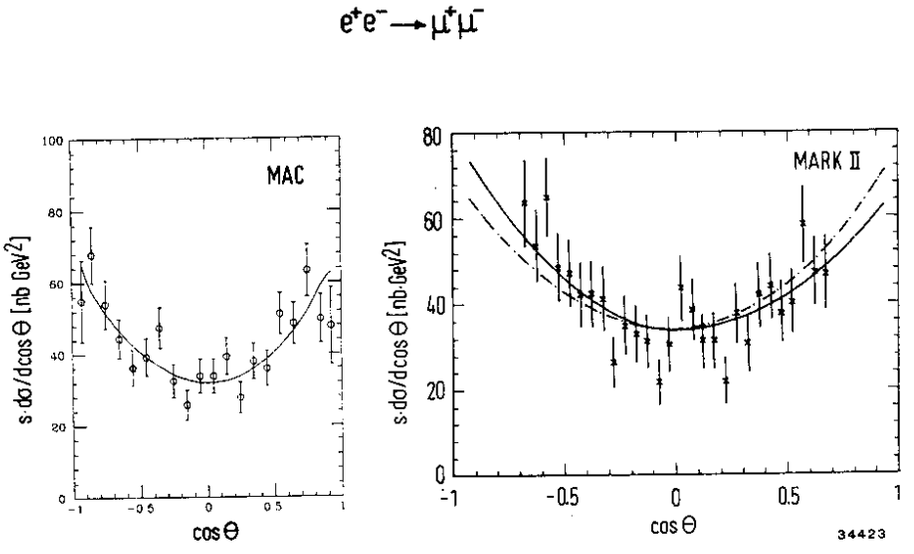
$e^+e^- \to \mu^+\mu^-$
MAC
MARK II
s·dσ/dcosΘ [nb GeV²]
cosΘ
34423

Fig. 5b

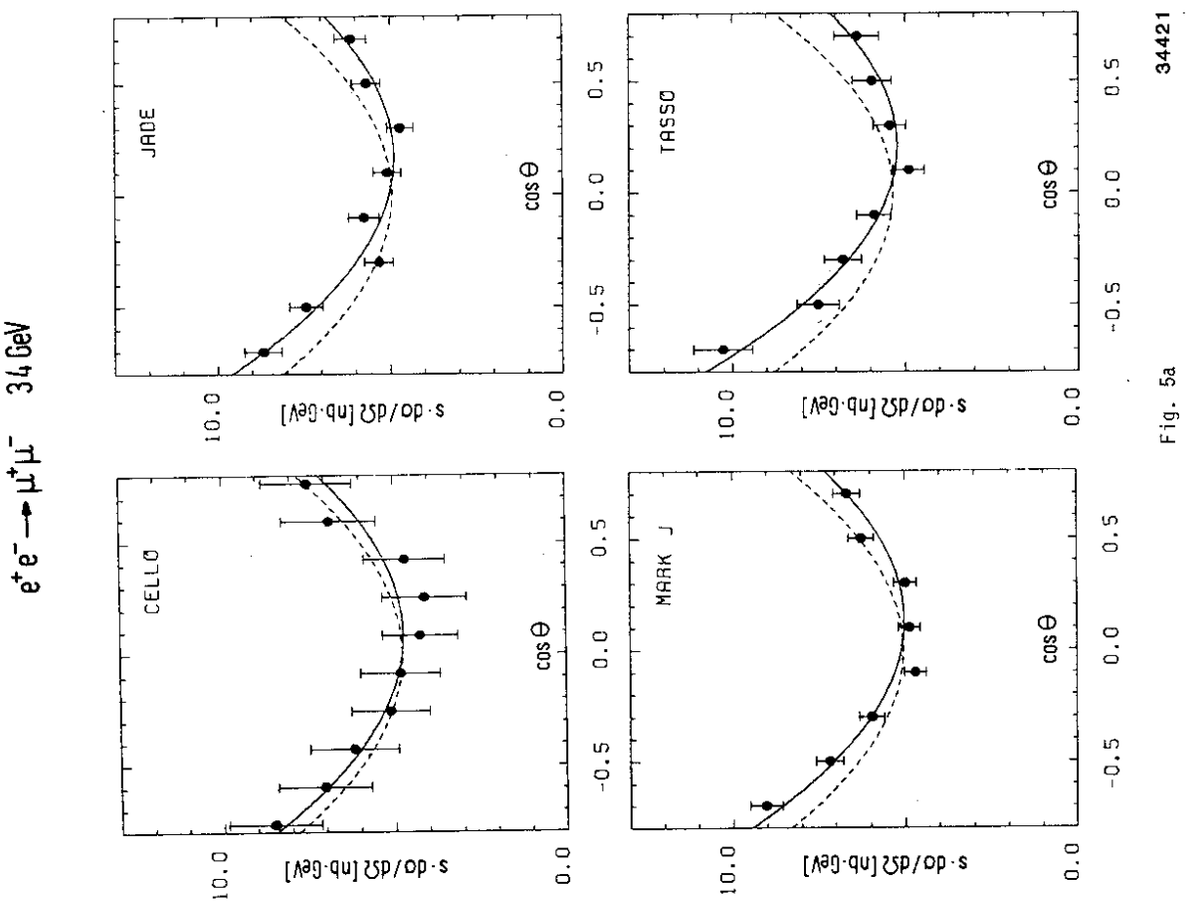
$e^+e^- \to \mu^+\mu^-$ 34 GeV
JADE
TASSO
CELLO
MARK J
s·dσ/dΩ [nb·GeV]
cosΘ
34421

Fig. 5a

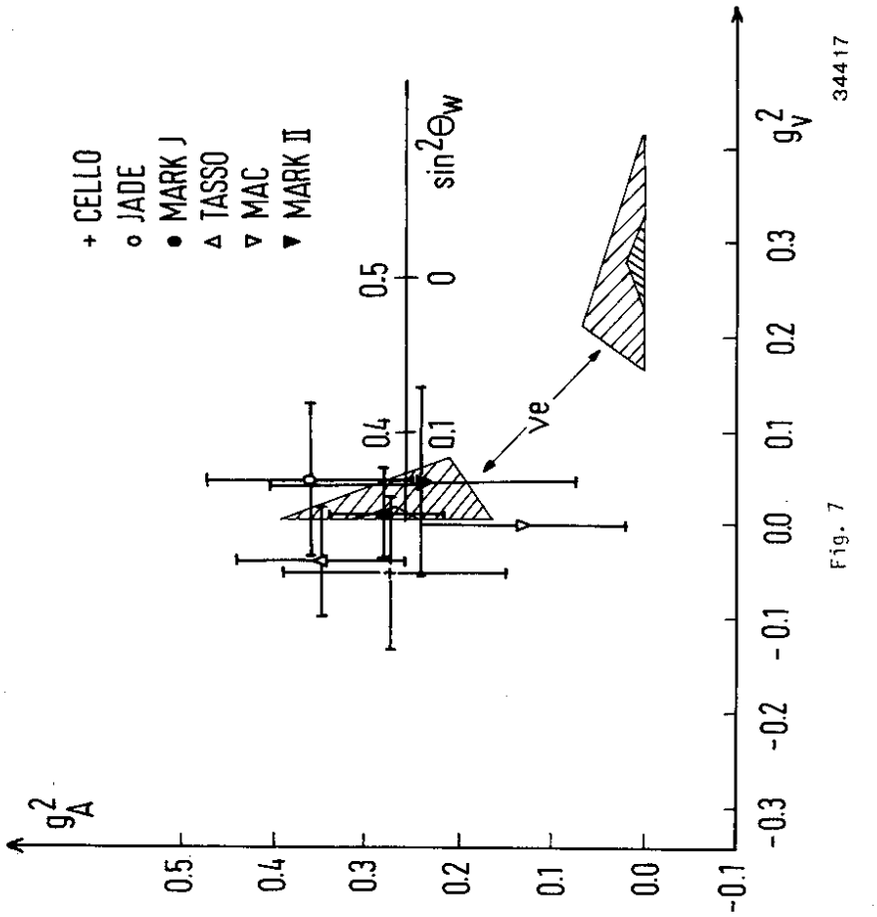
+ CELLO
o JADE
• MARK J
Δ TASSO
▽ MAC
▼ MARK II
$\sin^2\Theta_W$
0.5
0
0.4
0.1
νe
g_A^2
0.5
0.4
0.3
0.2
0.1
0.0
-0.1
g_V^2
0.3
0.2
0.1
0.0
-0.1
-0.2
-0.3
34417

Fig. 7

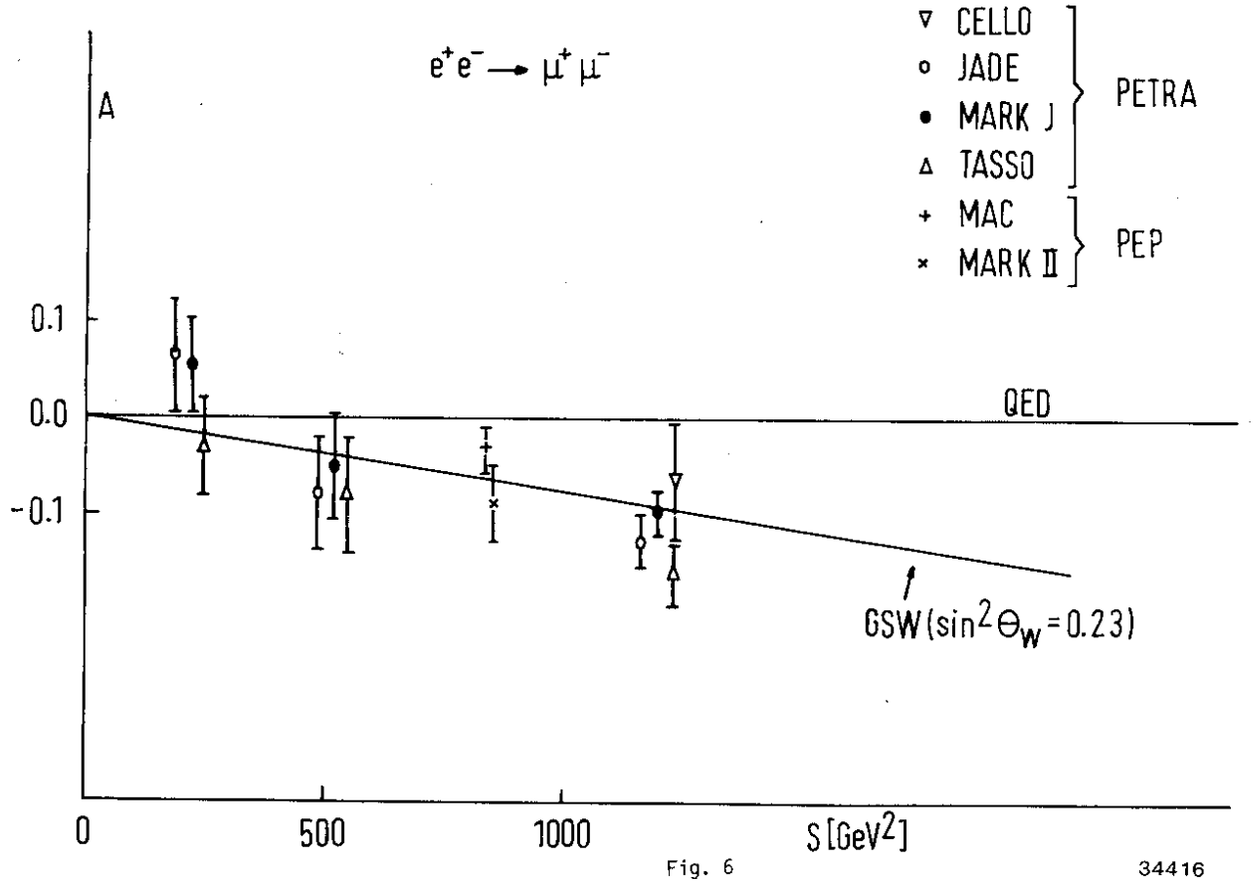
$e^+e^- \rightarrow \mu^+\mu^-$
A
▽ CELLO
o JADE
• MARK J
Δ TASSO
PETRA
+ MAC
× MARK II
PEP
0.1
0.0
-0.1
QED
GSW ($\sin^2\Theta_W = 0.23$)
0
500
1000
S [GeV^2]
34416

Fig. 6

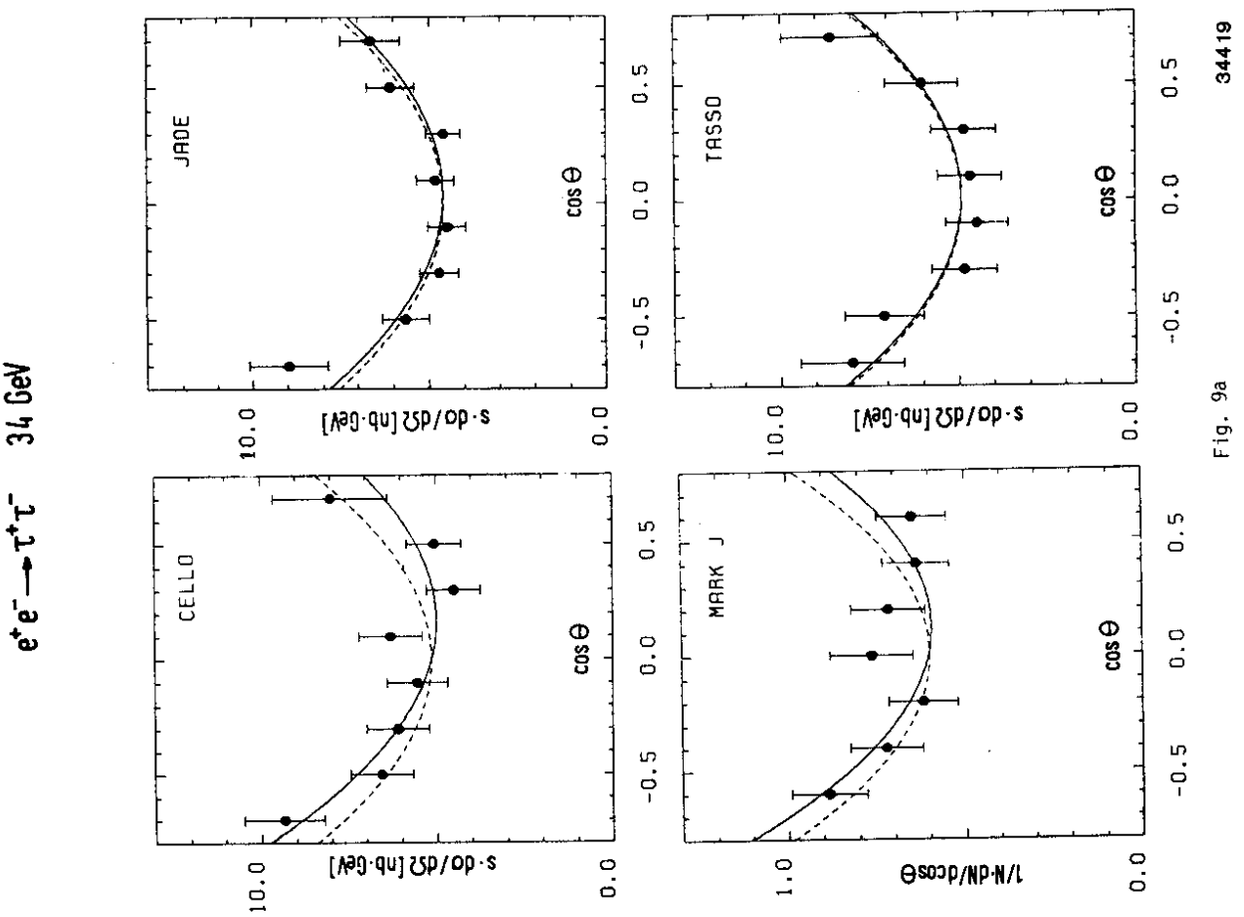
$e^+e^- \rightarrow \tau^+\tau^-$ 34 GeV
JADE
TASSO
CELLO
MARK J
cos Θ
s·dσ/dΩ [nb·GeV]
1/N·dN/dcosΘ
34419

Fig. 9a

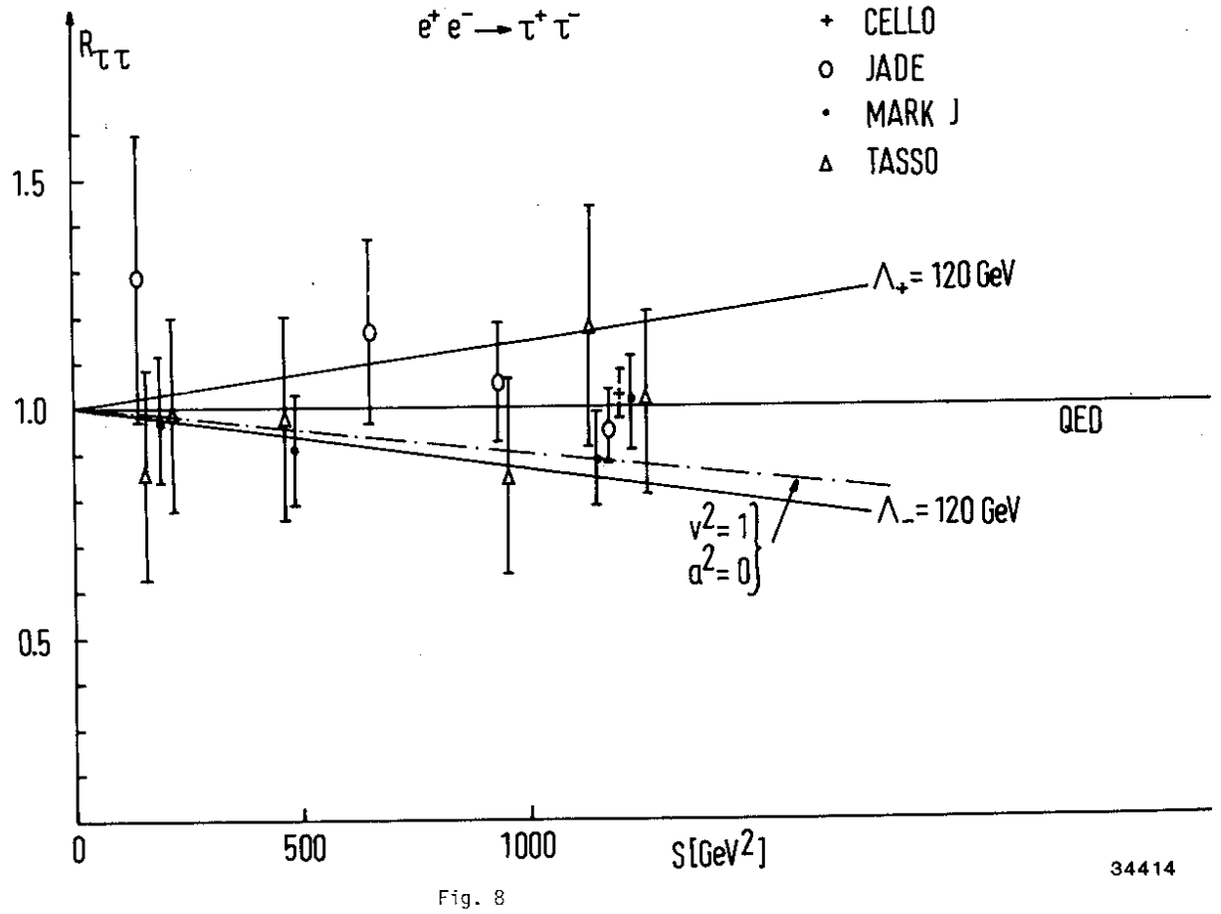
$e^+e^- \rightarrow \tau^+\tau^-$
$R_{\tau\tau}$
CELLO
JADE
MARK J
TASSO
$\Lambda_+ = 120$ GeV
QED
$\Lambda_- = 120$ GeV
$v^2 = 1$
$a^2 = 0$
S[GeV^2]
34414

Fig. 8

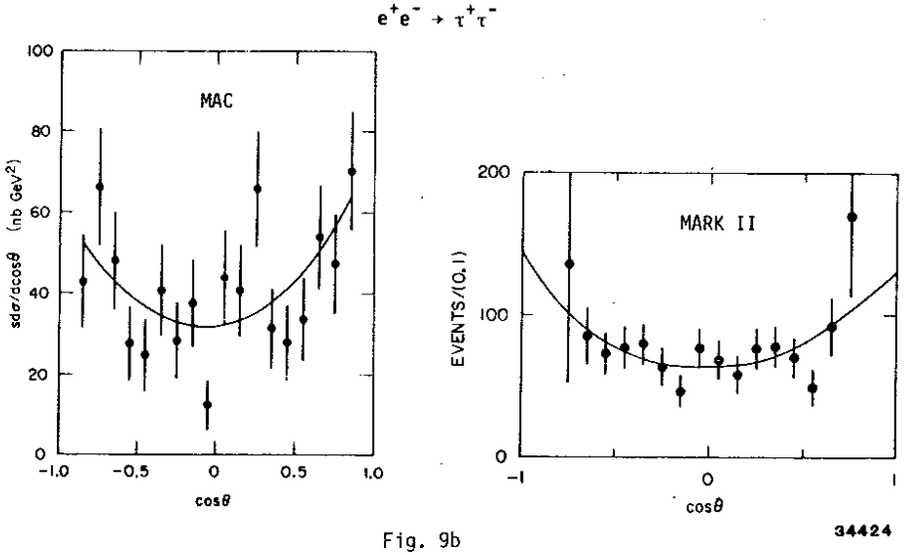

Fig. 9b

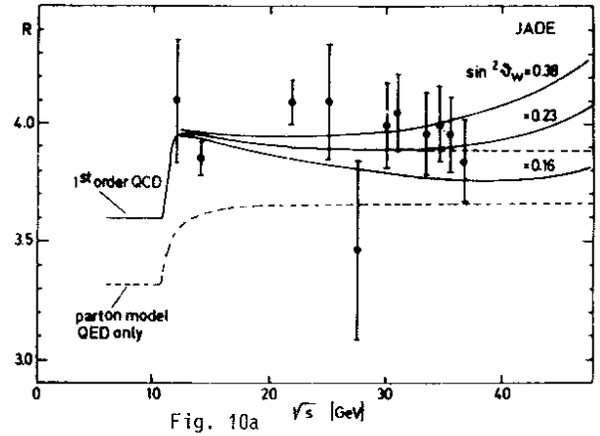

Fig. 10a

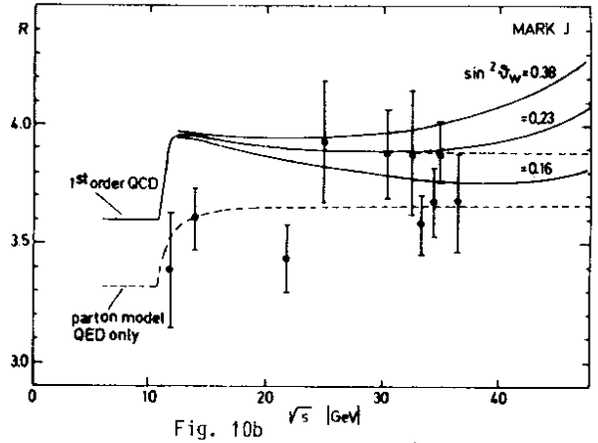

Fig. 10b

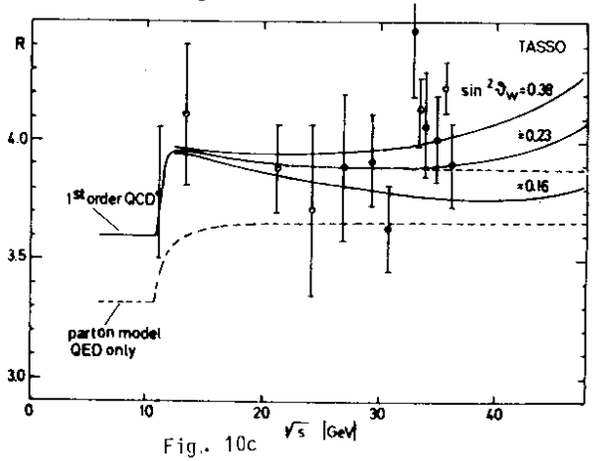

Fig. 10c

34422